



LAWRENCE  
LIVERMORE  
NATIONAL  
LABORATORY

# Activation Energy of Tantalum-Tungsten Oxide Thermite Reaction

Octavio Cervantes, Joshua Kuntz, Alex Gash,  
Zuhair Munir

March 3, 2010

Combustion and Flame

## **Disclaimer**

---

This document was prepared as an account of work sponsored by an agency of the United States government. Neither the United States government nor Lawrence Livermore National Security, LLC, nor any of their employees makes any warranty, expressed or implied, or assumes any legal liability or responsibility for the accuracy, completeness, or usefulness of any information, apparatus, product, or process disclosed, or represents that its use would not infringe privately owned rights. Reference herein to any specific commercial product, process, or service by trade name, trademark, manufacturer, or otherwise does not necessarily constitute or imply its endorsement, recommendation, or favoring by the United States government or Lawrence Livermore National Security, LLC. The views and opinions of authors expressed herein do not necessarily state or reflect those of the United States government or Lawrence Livermore National Security, LLC, and shall not be used for advertising or product endorsement purposes.

## Activation Energy of Tantalum-Tungsten Oxide Thermite Reactions

*Octavio G. Cervantes<sup>1,2</sup>, Joshua D. Kuntz<sup>1</sup>, Alexander E. Gash<sup>1</sup>, and Zuhair A. Munir<sup>1,2</sup>*

<sup>1</sup>Physical and Life Sciences Directorate, Lawrence Livermore National Laboratory, 7000 East Ave, Livermore, CA 94550, USA

<sup>2</sup>Chemical Engineering & Materials Science, University of California, One Shields Ave, Davis, CA 95616, USA

### **ABSTRACT**

The activation energy of a high melting temperature sol-gel (SG) derived tantalum-tungsten oxide thermite composite was determined using the Kissinger isoconversion method. The SG derived powder was consolidated using the High Pressure Spark Plasma Sintering (HPSPS) technique to 300 and 400°C to produce pellets with dimensions of 5 mm diameter by 1.5 mm height. A custom built ignition setup was developed to measure ignition temperatures at high heating rates (500 – 2000°C·min<sup>-1</sup>). Such heating rates were required in order to ignite the thermite composite. Unlike the 400°C samples, results show that the samples consolidated to 300°C undergo an abrupt change in temperature response prior to ignition. This change in temperature response has been attributed to the crystallization of the amorphous WO<sub>3</sub> in the SG derived Ta-WO<sub>3</sub> thermite composite and not to a pre-ignition reaction between the constituents. Ignition temperatures for the Ta-WO<sub>3</sub> thermite ranged from approximately 465 – 670°C. The activation energy of the SG derived Ta-WO<sub>3</sub> thermite composite consolidated to 300 and 400°C were determined to be 37.787 ± 1.58 kJ·mol<sup>-1</sup> and 57.381 ± 2.26 kJ·mol<sup>-1</sup>, respectively.

### **INTRODUCTION**

In 1895, German chemist Hans Goldschmidt patented the oxidation/reduction or redox reaction between a metal and a metal oxide, a reaction which has been referred as thermite [1]. A typical thermite reaction is between aluminum and iron oxide,



As indicated by Eq (1), thermite reactions are exothermic which can be self-sustaining. Their mechanism and utilization have been described in detail elsewhere [2]. Because of the high thermodynamic stability of its oxide ( $Al_2O_3$ ,  $\Delta H_f = -1675.7 \text{ kJ}\cdot\text{mol}^{-1}$  at  $25^\circ\text{C}$ ) and its low melting temperature ( $660^\circ\text{C}$ ), aluminum has been widely used as the fuel metal in combination with various oxides such as  $Fe_2O_3$ ,  $CuO$ ,  $MoO_3$  and  $WO_3$  [3-10]. Important kinetic parameters such as ignition and peak temperatures as a function of heating rate are obtained from differential thermal analysis (DTA) and differential scanning calorimetry (DSC) measurements. These temperatures may in turn be used to determine the activation energy of the thermite as a function of a particular parameter of interest (e.g., particle size or distribution).

Determining the activation energy of thermite composites is an important parameter of the ignition process. Such activation energy is defined as the minimum amount of energy required to initiate the reaction between the thermite constituents. Studies have been conducted to determine the activation energy of Al-based thermite composites using isoconversion processing of heat flow data as a function of temperature for various heating rates from DSC measurements [4, 11-13]. In other studies the activation energy of Al-based intermetallic energetic materials was determined using isoconversion methods from temperature versus time thermograms in laser ignition experiments [14, 15].

The laser ignition of energetic materials is a nonisothermal analysis that supplies a constant heat flux to the sample of interest. Such analysis assumes that the ignition temperature corresponds to a fixed state of transformation of the compound from reactants to products. This nonisothermal analysis may be applied to determine the activation energy,  $E_A$ , of energetic materials as long as the thermograms are reproducible and depict specific ignition temperatures [14].

There are a number of isoconversion methods [16-20] that have been applied to determine  $E_A$ . According to the Kissinger isoconversion method [16],  $E_A$  may be calculated from

$$\frac{d \ln \left[ \frac{\beta}{T_{ign}^2} \right]}{dT} = - \frac{E_A}{R} \quad (2)$$

where  $\beta$  is the heating rate,  $T_{ign}$  is the ignition temperature,  $R$  is the universal gas constant and  $T$  is the absolute temperature. The activation energy,  $E_A$ , is obtained from the slope of an Arrhenius plot of  $\ln [\beta / T_{ign}^2]$  vs.  $1/T$ .

As indicated above, several isoconversion methods have been employed to determine  $E_A$ , for Al-based thermite reactions from DSC, DTA, and laser ignition measurements [11-15, 21-23]. To our knowledge, we do not know of any studies done on the determination of  $E_A$  for thermites with a high melting temperature ( $\sim 3000^\circ\text{C}$ ) as a fuel metal. Here we present results of an investigation on the activation energy of a sol-gel derived Ta-WO<sub>3</sub> thermite reaction. The Kissinger isoconversion method was applied in this study since it has also been previously used on laser ignition studies of intermetallic energetic composites [14, 15].

## EXPERIMENTAL METHODS

### A. Materials Synthesis

A Ta-WO<sub>3</sub> thermite composite powder was prepared using sol-gel techniques. The synthesis of the reactive composite is described in detail elsewhere [24]. Here we provide a brief description of the process, 14.76 g (43.5 mmol) of WOCl<sub>4</sub> (F.W. = 339 g mol<sup>-1</sup>; 98% from Sigma-Aldrich, Milwaukee, WI) were dissolved in 125 mL ethanol/H<sub>2</sub>O solution with a 95/5 vol % composition. After filtering the solution, 9.2 g (52.2 mmol) of capacitor grade Ta metal powder (H.C. Starck; average particle size 5  $\mu\text{m}$  and 99.99% pure) was added to the filtered solution to make a composite mixture. While stirring the mixture, 20 g (235 mmol) of 3,3,-dimethyloxetane (DMO) (98% pure from Sigma-

Aldrich, Milwaukee, WI) was added to the mixture. Shortly thereafter, a gelation of a uniform composite occurred. This method provides an energetic composite that incorporates immobilized micrometric tantalum in a three-dimensional nanostructured tungsten oxide gel with a 6:5 (Ta:WO<sub>3</sub>) mole ratio as shown in Eq. (3).



### ***B. Consolidation of Sol-Gel Ta-WO<sub>3</sub>***

The consolidation of the sol-gel Ta-WO<sub>3</sub> energetic composites was performed using the high-pressure spark plasma sintering (HPSPS) method. Details on this technique are presented elsewhere [25, 26]. It is similar to hot-pressing with the distinct difference that the heating is effected by a pulsed DC current applied to the sample and the graphite die. The graphite die assembly is made up of several internal components that allows for the application of pressures as high as 1 GPa. Graphite dies with a 5 mm inner diameter were used to consolidate the samples at 300 and 400°C. An initial pressure of 150 MPa was applied to the samples which were heated from room temperature to 200°C at approximately 50°C·min<sup>-1</sup>. In order to remove any residual solvents or physically adsorbed water, the samples were held at 200°C for 2 min. During the 2-min hold, the pressure was increased to 300 MPa and the temperature increased at a rate of approximately 100°C·min<sup>-1</sup> to the desired final temperature. Once at temperature, the sample was held there for 3 min. The average sample weight and dimensions were 0.225 ± 0.005 g and 5 ± 0.1 mm diameter by 1.5 ± 0.3 mm height.

### ***C. Ignition Setup***

The development of a custom built ignition setup was necessary since conventional DSC apparatus were not capable of generating the required heating rates to initiate the thermite reaction and since experimental problems were encountered during laser ignition experiments. Laser ignition experiments have been previously applied to the ignition of intermetallic energetic composites [14, 15], therefore laser ignition experiments were attempted to ignite the Ta-WO<sub>3</sub> thermite reaction. The laser

experiments generated the required heating rates and initiated the composite, but after many attempts we were not able to obtain reproducible data. We found that the thermite sample spalls and disperses away during the laser ignition experiments making it difficult to monitor the temperature profile of the sample. As a result, we developed an in-house custom designed apparatus which provided the required heating rates (500 – 2000°C·min<sup>-1</sup>) and generated reproducible data. In our experimental setup a laser is not used to provide a constant heat flux, instead the sample is exposed to a constant radiant heat flux provided by filament wires capable of generating reproducible thermograms and specific ignition temperatures.

Our experimental setup consisted of placing a 50 mm diameter quartz tube in a tube furnace operating at temperatures ranging from 800 to 1000°C depending on the desired heating rate. One end of the tube furnace was capped with a fitting to allow inert gas to flow through the tube. The other end of the tube remained open to allow for the insertion of a smaller (~ 25 mm diameter) quartz tube assembly (see Figure 1 (a)). The smaller tube (Figure 1 (b)) was likewise capped on one end by a fitting to hold the 25 mm quartz tube in place, fasten an alumina tube and allow for inert gas to flow during the ignition experiments. The sample was assembled by attaching a 0.127 mm K-type thermocouple to the top surface of the sample using conductive silver ink (Alfa Aesar, Ward Hill, MA). The sample was then covered with a 0.6 mm thick zirconia blanket to moderate the heat flow to the sample (Figure 1 (c)). The thermocouple with the attached sample and zirconia blanket were then inserted through an alumina tube containing two ports for each of the thermocouple leads. Argon gas was purged at 300 mL·min<sup>-1</sup> during the experiment. Figure 1 (d) shows a schematic of a fully assembled experimental setup.

At least 10 samples at each consolidation temperature (300 and 400°C) were tested using the described experimental setup. Temperature versus time data were collected at an average rate of 36  $\mu$ s per data point using an Agilent 34970A Data Acquisition/Switch Unit. Heating rates varied from 500 to 2000°C·min<sup>-1</sup>.

## RESULTS AND DISCUSSIONS

### *A. Ignition Thermograms and Activation Energy*

Typical thermograms of samples consolidated at 300 and 400°C by the HPSPS method are presented in Figure 2. It can be observed that the temperature profile for the sample consolidated at 300°C is different from that of the sample consolidated at 400°C. The sample consolidated at 300°C shows a shoulder in the temperature profile prior to the final rise associated with the ignition of the reaction. In contrast, the sample consolidated at 400°C does not show a similar change in the temperature profile prior to ignition.

The heating rates and the ignition temperatures for each sample were calculated and determined using their corresponding thermograms. Since the 300°C samples displayed a shoulder in the temperature response prior to ignition, two heating rates and two ignition temperatures were calculated and determined for each sample. The first heating rate was calculated for the temperature rise from room temperature to the beginning of the temperature shoulder (labeled as Slope 1 in Figure 2). The first ignition temperature was determined from the intersection of a tangent line between Slope 1 and Slope 2 (Slope 2 represents the initial part of the shoulder, as shown in Figure 2). The first heating rate and ignition temperature for the 300°C samples in Figure 2 were calculated and determined to be approximately  $588^{\circ}\text{C}\cdot\text{min}^{-1}$  and  $478^{\circ}\text{C}$ . From herethereafter we will refer to this as the 1<sup>st</sup> ignition data for the 300°C thermograms. The second heating rate was calculated from Slope 3 as indicated in Figure 2. The second ignition temperature was determined from the intersection of a tangent line drawn between Slope 3 and Slope 4. The second heating rate and ignition temperature for the 300°C samples in Figure 2 were determined to be approximately  $927^{\circ}\text{C}\cdot\text{min}^{-1}$  and  $533^{\circ}\text{C}$ . From herethereafter we will refer to this as the 2<sup>nd</sup> ignition data for the 300°C thermograms.

The same methodology was applied to calculate and determine the heating rate and ignition temperature for the 400°C samples. The difference between the 300°C and the

400°C samples is that for the 400°C samples only one heating rate and one ignition temperature were determined. Such distinction was necessary since these samples do not undergo a distinct change in temperature response prior to ignition. The heating rate and ignition temperature for the 400°C samples in Figure 2 were calculated to be about  $505^{\circ}\text{C}\cdot\text{min}^{-1}$  and  $551^{\circ}\text{C}$ .

Heating rates generated from our in-house experimental setup to initiate the Ta-WO<sub>3</sub> thermite reaction ranged from about 500 to  $2000^{\circ}\text{C}\cdot\text{min}^{-1}$  and the ignition temperatures ranged from approximately 465 to  $670^{\circ}\text{C}$ . All of the resulting heating rates and ignition temperatures were applied to the Kissinger isoconversion method to determine the activation energy,  $E_A$ , of the samples consolidated at each temperature. Table 1 shows the activation energy values for SG derived Ta-WO<sub>3</sub> samples consolidated at 300 and  $400^{\circ}\text{C}$ .

It can be seen from the root mean square values, the uncertainty in the calculated activation energy for the first ignition data is high. We postulate that this uncertainty may be related to complex pre-ignition reactions between the constituents. Pre-ignition reactions have been verified by previous observations in intermetallic energetic composites [27].

### ***B. Ignition Quench of Consolidated 300°C Sol-Gel Ta-WO<sub>3</sub>***

To investigate if pre-ignition reactions do occur in the samples consolidated at  $300^{\circ}\text{C}$ , partially converting of the reactants of the SG derived Ta-WO<sub>3</sub> powders to products or intermediate phases, quenching experiments were carried out. Figure 3 shows the XRD patterns of (a) the starting SG derived Ta-WO<sub>3</sub> powder mixture, (b) the sample consolidated at  $300^{\circ}\text{C}$ , (c) consolidated at  $400^{\circ}\text{C}$ , and (d) a non-consolidated (as-received) powder mixture of a commercially available WO<sub>3</sub> and Ta. The x-ray diffraction patterns show that the WO<sub>3</sub> in the SG derived Ta-WO<sub>3</sub> composite is amorphous as the pattern only shows Ta peaks. In contrast and as expected, the XRD pattern of the powder mixture of the commercially available WO<sub>3</sub> and Ta shows that both constituents

are crystalline. In addition, the sample consolidated at 300°C shows minor peaks of tantalum suboxide indicative of pre-ignition reaction between the constituents. The Ta suboxide that best fits these peaks is in the form of  $TaO_x$  as presented by Brauer, et. al [28]. Furthermore, Figure 3 (c) shows that the  $WO_3$  remains amorphous. In contrast, the XRD of the sample consolidated at 400°C shows a higher degree of pre-ignition reaction between the Ta and the  $WO_3$  as can be seen by the intensity of the tantalum suboxide peaks, Figure 3 (c). In this case, there is evidence of the initiation of the crystallization of the amorphous  $WO_3$  as depicted by the two peaks labeled  $WO_3$  in the XRD pattern (Figure 3 (c)).

To investigate the sequence of phase formation in the thermite reaction, samples were quenched by rapidly removing them from the tube furnace prior to ignition. Figure 4 shows typical thermograms of the sample sintered at 300°C. Curve 1 is the typical temperature profile for an unquenched sample while curve 2 shows a thermogram of the quenched sample. The quenching (quick removal of the sample from the hot zone) resulted in the avoidance of the main combustion reaction. The approximate heating and cooling rates for this sample were  $590^\circ\text{C}\cdot\text{min}^{-1}$  and  $335^\circ\text{C}\cdot\text{min}^{-1}$ , respectively. To be used as a reference point, Figure 5 (a) shows the XRD pattern of the SG derived Ta- $WO_3$  sample consolidated to 300°C. It can be observed that it is composed of crystalline Ta,  $TaO_x$  and amorphous  $WO_3$ . Figure 5 (b) presents the XRD pattern of the quenched SG derived Ta- $WO_3$  sample consolidated to 300°C. XRD analysis of the quenched sample showed evidence of crystallization of the amorphous  $WO_3$  as depicted by the two peaks labeled as  $WO_3$ , but no significant evidence of pre-ignition reaction, as seen in Figure 5 (b).

Furthermore, when the quenched sample (curve 2, Figure 4) was exposed to the same heat conditions for a second time and allowed to ignite (curve 3, Figure 4), it becomes apparent that the thermogram does not have a distinct temperature shoulder prior to ignition as the 300°C samples typically show. It is important to point out that the ignition time of the quenched sample (curve 3, Figure 4) is about 0.2 min (12 sec) longer than

the unquenched sample (curve 1, Figure 4). We postulate that the crystallization of the amorphous  $\text{WO}_3$  is an exothermic event that acts as an internal heat source for the reaction to initiate. The rapid increase in temperature shown in the thermogram (curve 1, Figure 4) during the crystallization of the  $\text{WO}_3$  decreases the ignition times of an unquenched sample (curve 1, Figure 4) in comparison to a quenched sample (curve 3, Figure 4). Therefore, it is important to note that abrupt change in temperature response (or temperature shoulder) prior to ignition observed in the thermograms for 300°C Ta- $\text{WO}_3$  samples is not due to a pre-ignition reaction between the Ta and the  $\text{WO}_3$ , but instead is due to the crystallization of  $\text{WO}_3$  as shown by the x-ray diffraction patterns in Figure 5 (b).

### ***C. Ignition Quench of Sol-Gel Amorphous $\text{WO}_3$***

To verify that the temperature shoulder response in the 300°C SG Ta- $\text{WO}_3$  samples was due to the crystallization of  $\text{WO}_3$ , several sol-gel amorphous  $\text{WO}_3$  samples were consolidated (300°C) using the HPSPS to compare to the SG Ta- $\text{WO}_3$  samples. From such consolidation runs, it was learned that such  $\text{WO}_3$  samples are difficult to consolidate and crystallize during consolidation, hence we are not able to compare the SG derived Ta- $\text{WO}_3$  samples to sol-gel amorphous  $\text{WO}_3$  under similar consolidation conditions. However, quenching a pressed (25°C) sol-gel amorphous  $\text{WO}_3$  sample is acceptable since the sample remains amorphous and we are able to obtain cylindrical samples. Figure 6 shows the thermograms of the quenched SG Ta- $\text{WO}_3$  with a cooling rate of 335°C·min<sup>-1</sup> and the sol-gel amorphous  $\text{WO}_3$  sample with a cooling rate of 225°C·min<sup>-1</sup>. It can be observed that both samples were quenched at the same temperature; therefore we are able to compare their crystal structure.

It is important to note that the difference in heating rate between the SG derived Ta- $\text{WO}_3$  composite and the amorphous  $\text{WO}_3$  in Figure 6 may be attributed to differences in thermal conductivity of each sample. During the experiment, the  $\text{WO}_3$  will respond slower to the heating as it lacks the thermal response of the Ta. Moreover, the

difference may be attributed to the fact that the  $\text{WO}_3$  is a porous three-dimensional nanostructure network whose convective heat transfer will be the rate limiting factor. The XRD pattern of the quenched  $\text{WO}_3$  shows that the  $\text{WO}_3$  has begun to crystallize as shown in Figure 5 (c), this pattern is very similar to the one presented for the quenched Ta- $\text{WO}_3$  in Figure 5 (a). This supports the idea that the temperature shoulder on the 300°C samples may be due to the crystallization of  $\text{WO}_3$  and not a pre-ignition reaction between the reactants.

#### ***D. Consolidation and Ignition of Ta- $\text{WO}_3$ powder mixture with Crystalline $\text{WO}_3$***

To further explore the idea that the temperature shoulder on the 300°C SG derived Ta- $\text{WO}_3$  samples, several attempts were made to consolidate a Ta- $\text{WO}_3$  energetic composite composed with crystalline  $\text{WO}_3$  instead of the amorphous  $\text{WO}_3$ . In five attempts, only two Ta- $\text{WO}_3$  samples with crystalline  $\text{WO}_3$  with similar masses as the samples made with the amorphous  $\text{WO}_3$  were produced under similar consolidation conditions. Therefore, from a consolidation point of view, the composite with the amorphous  $\text{WO}_3$  consolidates much better than the composite with the crystalline  $\text{WO}_3$ . The composite with the amorphous  $\text{WO}_3$  always produces good samples after each consolidation run. Since consolidating the Ta- $\text{WO}_3$  composite with the crystalline  $\text{WO}_3$  was difficult, ignition experiments were performed with smaller mass samples ( $\leq 0.1$  g instead of the common 0.225 g). It was found that such samples react, but do not ignite under the lowest heating setting (furnace at 800°C). Instead in order to ignite these samples the furnace was set to 1000°C, which is the highest temperature setting used in these ignition experiments.

Ta- $\text{WO}_3$  samples with crystalline  $\text{WO}_3$  of approximately 0.225 g were ignition tested while setting the furnace to 1000°C. Results show (as seen in Figure 7) that the ignition of the Ta- $\text{WO}_3$  with crystalline  $\text{WO}_3$  does not exhibit the abrupt change in temperature response prior to ignition as previously observed in the SG derived Ta- $\text{WO}_3$  samples consolidated to 300°C. It is believed that since the  $\text{WO}_3$  is already crystalline, it does

not undergo the amorphous to crystalline transformation as the SG derived Ta-WO<sub>3</sub> samples do. Hence the absence on the temperature shoulder in the thermogram.

These results further support the notion that the abrupt change in temperature response prior to ignition in the Ta-WO<sub>3</sub> samples with the amorphous WO<sub>3</sub> crystallizes prior to ignition. Furthermore, Figure 7 shows that the ignition of the Ta-WO<sub>3</sub> with the crystalline WO<sub>3</sub> occurs at about 800°C which is about 150°C higher than the Ta-WO<sub>3</sub> with amorphous WO<sub>3</sub> under similar heating conditions. In addition, it is important to note that the ignition time for both samples is very similar. This indicates that at under these heating rates, the amount of heat required to ignite these thermite composites is about the same regardless of the crystal structure of the reactants.

## CONCLUSIONS

The activation energy of a high melting temperature tantalum-tungsten oxide thermite composite has been determined using the Kissinger isoconversion method. Powder samples were consolidated using the High Pressure Spark Plasma Sintering (HPSPS) technique to 300 and 400°C. A custom built ignition setup was developed to measure ignition temperatures at high heating rates (500 – 2000°C·min<sup>-1</sup>). Such heating rates were required in order to ignite the thermite composite. Unlike the 400°C samples, results show that the samples consolidated to 300°C undergo an abrupt change in temperature response prior to ignition. This change in temperature response has been attributed to the crystallization of the amorphous WO<sub>3</sub> in the sol-gel derived Ta-WO<sub>3</sub> thermite composite and not to a pre-ignition reaction between the constituents. Ignition temperatures for the Ta-WO<sub>3</sub> thermite ranged from approximately 465 – 670°C. The ignition of Ta-WO<sub>3</sub> with amorphous WO<sub>3</sub> generally occurs at lower temperatures than the Ta-WO<sub>3</sub> composite with the crystalline WO<sub>3</sub>. It is postulated that the crystallization of the amorphous WO<sub>3</sub> provides sufficient energy to ignite the 300°C samples at lower temperatures. Moreover, it was found that the amorphous WO<sub>3</sub> used in this study, crystallizes while consolidating the powder under the same conditions as the Ta-WO<sub>3</sub>

thermite composite. This indicates that the consolidation mechanism of the Ta-WO<sub>3</sub> and the sol-gel amorphous WO<sub>3</sub> are different. In contrast to the Ta-WO<sub>3</sub> with amorphous WO<sub>3</sub>, in which a good pellet is produced after each consolidation run, the Ta-WO<sub>3</sub> with crystalline WO<sub>3</sub> is difficult to consolidate under the same conditions. Therefore, from a large production point of view, one may suggest to use the sol-gel derived Ta-WO<sub>3</sub> instead of the Ta-WO<sub>3</sub> with crystalline WO<sub>3</sub>.

## ACKNOWLEDGEMENTS

This work performed under the auspices of the U.S. Department of Energy by Lawrence Livermore National Laboratory under Contract DE-AC52-07NA27344. The authors are grateful to the Joint DoD/DOE Munitions Technology Development Program for funding this project. Special thanks to graduate student Steven Dean and Professor Michelle Pantoya at Texas Tech University for their assistance and collaboration on the laser ignition experiments.

## REFERENCES

1. Goldschmidt, H. 1895: German Patent 96,317.
2. Wang, L.L., Z.A. Munir, and Y.M. Maximov, *Thermite Reactions - Their Utilization in the Synthesis and Processing of Materials*. Journal of Materials Science, 1993. **28**(14): p. 3693-3708.
3. Umbrajkar, S.M., et al. *Aluminum-rich Al-MoO<sub>3</sub> nanocomposite powders prepared by arrested reactive milling*. in *AIAA 45th Aerospace Sciences Meeting and Exhibit*. 2007. Reno, NV: Amer Inst Aeronaut Astronaut.
4. Pantoya, M.L. and J.J. Granier. *The effect of slow heating rates on the reaction mechanisms of nano and micron composite thermite reactions*. in *33rd Annual Meeting of the North-American-Thermal-Analysis-Society*. 2005. Univ City, CA: Springer.
5. Moore, K. and M.L. Pantoya, *Combustion of environmentally altered molybdenum trioxide nanocomposites*. Propellants Explosives Pyrotechnics, 2006. **31**(3): p. 182-187.
6. Prentice, D., M.L. Pantoya, and A.E. Gash, *Combustion wave speeds of sol-gel-synthesized tungsten trioxide and nano-aluminum: The effect of impurities on flame propagation*. Energy & Fuels, 2006. **20**(6): p. 2370-2376.
7. Plantier, K.B., M.L. Pantoya, and A.E. Gash, *Combustion wave speeds of nanocomposite Al/Fe<sub>2</sub>O<sub>3</sub>: the effects of Fe<sub>2</sub>O<sub>3</sub> particle synthesis technique*. Combustion and Flame, 2005. **140**(4): p. 299-309.
8. Schoenitz, M., S. Umbrajkar, and E.L. Dreizin, *Kinetic analysis of thermite reactions in Al-MoO<sub>3</sub> nanocomposites*. Journal of Propulsion and Power, 2007. **23**(4): p. 683-687.

9. Son, S.F., et al., *Combustion of nanoscale Al/MoO<sub>3</sub> thermite in microchannels*. Journal of Propulsion and Power, 2007. **23**(4): p. 715-721.
10. Umbrajkar, S.M., M. Schoenitz, and E.L. Dreizin, *Exothermic reactions in Al-CuO nanocomposites*. Thermochemica Acta, 2006. **451**(1-2): p. 34-43.
11. Sun, J., M.L. Pantoya, and S.L. Simon, *Dependence of size and size distribution on reactivity of aluminum nanoparticles in reactions with oxygen and MoO<sub>3</sub>*. Thermochemica Acta, 2006. **444**(2): p. 117-127.
12. Dyer, T. and Z. Munir, *The synthesis of nickel aluminides by multilayer self-propagating combustion*. Metallurgical and Materials Transactions B, 1995. **26**(3): p. 603-610.
13. Blobaum, K.J., et al., *Al/Ni formation reactions: characterization of the metastable Al<sub>9</sub>Ni<sub>2</sub> phase and analysis of its formation*. Acta Materialia, 2003. **51**(13): p. 3871-3884.
14. Hunt, E.M. and M.L. Pantoya, *Ignition dynamics and activation energies of metallic thermites: From nano- to micron-scale particulate composites*. Journal of Applied Physics, 2005. **98**(3): p. 034909.
15. Monagheddu, M., et al., *Ignition phenomena in combustion synthesis: An experimental methodology*. Journal of Applied Physics, 2002. **92**(1): p. 594-599.
16. Kissinger, H.E., *Reaction Kinetics in Differential Thermal Analysis*. Analytical Chemistry, 1957. **29**(11): p. 1702-1706.
17. Ozawa, T., Bull. Chem. Soc. Jpn., 1965. **38**: p. 1881.
18. Flynn, J.H. and L.A. Wall, J. Res. Nat. Bur. Standards, 1966. **70A**: p. 487.
19. Starink, M.J., *A new method for the derivation of activation energies from experiments performed at constant heating rate*. Thermochemica Acta, 1996. **288**(1-2): p. 97-104.
20. Vyazovkin, S., *Advanced isoconversional method*. Journal of Thermal Analysis and Calorimetry, 1997. **49**(3): p. 1493-1499.
21. Fan, R.H., et al., *Kinetics of thermite reaction in Al-Fe<sub>2</sub>O<sub>3</sub> system*. Thermochemica Acta, 2006. **440**(2): p. 129-131.
22. Wang, Y., et al., *Thermal performance investigation of core-shell Cu/Al micron-nano composites with WO<sub>3</sub>*. Acta Physico-Chimica Sinica, 2007. **23**(11): p. 1753-1759.
23. Umbrajkar, S.M., et al., *On problems of isoconversion data processing for reactions in Al-rich Al-MoO<sub>3</sub> thermites*. Thermochemica Acta, 2008. **477**(1-2): p. 1-6.
24. Kuntz, J.D., O.G. Cervantes, A.E. Gash, and Z.A. Munir, *Combustion and Flame*, 2009. **Accepted**.
25. Anselmi-Tamburini, U., J.E. Garay, and Z.A. Munir, *Fast low-temperature consolidation of bulk nanometric ceramic materials*. Scripta Materialia, 2006. **54**(5): p. 823-828.
26. Munir, Z.A., U. Anselmi-Tamburini, and M. Ohyanagi, *The effect of electric field and pressure on the synthesis and consolidation of materials: A review of the spark plasma sintering method*. Journal of Materials Science, 2006. **41**(3): p. 763-777.
27. Lee, S.-H., et al., *Effect of heating rate on the combustion synthesis of intermetallics*. Materials Science and Engineering A, 2000. **281**(1-2): p. 275-285.
28. Brauer, G., H. Muller, and G. Kuhner, *OXIDE DER TIEFTEMPERATUROXYDATION VON NIOB UND TANTAL*. Journal of the Less-Common Metals, 1962. **4**(6): p. 533-546.

**Table 1** Apparent activation energy values determined by the Kissinger isoconversion method to SG derived Ta-WO<sub>3</sub> samples consolidated at to 300 and 400°C

Consolidation Temperature [°C]	Activation Energy [kJ•mol <sup>-1</sup> ]	Root Mean Square
300	1st Ignition Data	7.544 ± 5.36
	2nd Ignition Data	37.787 ± 1.58
400		57.381 ± 2.26

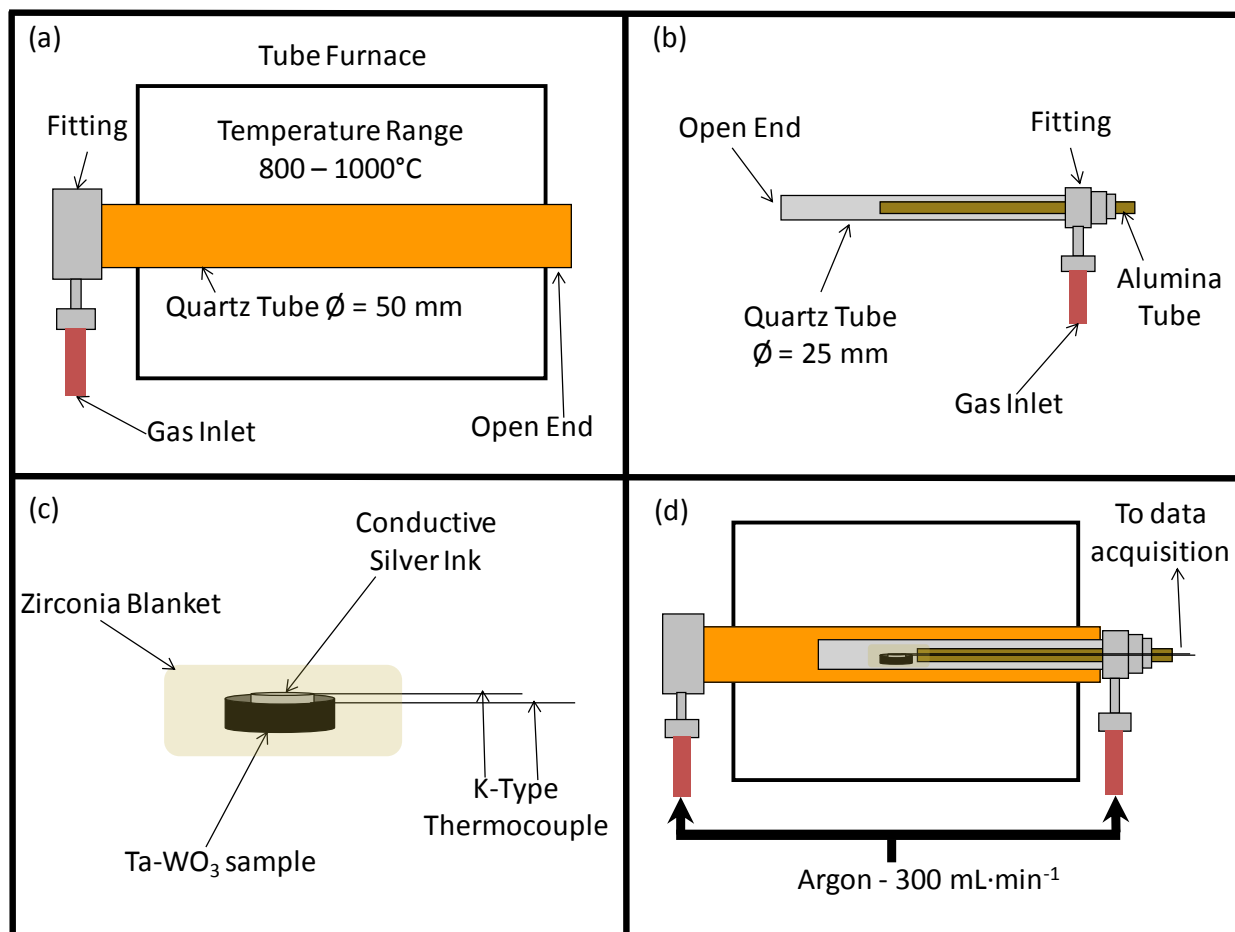


Figure 1. Schematic representation of experimental setup.

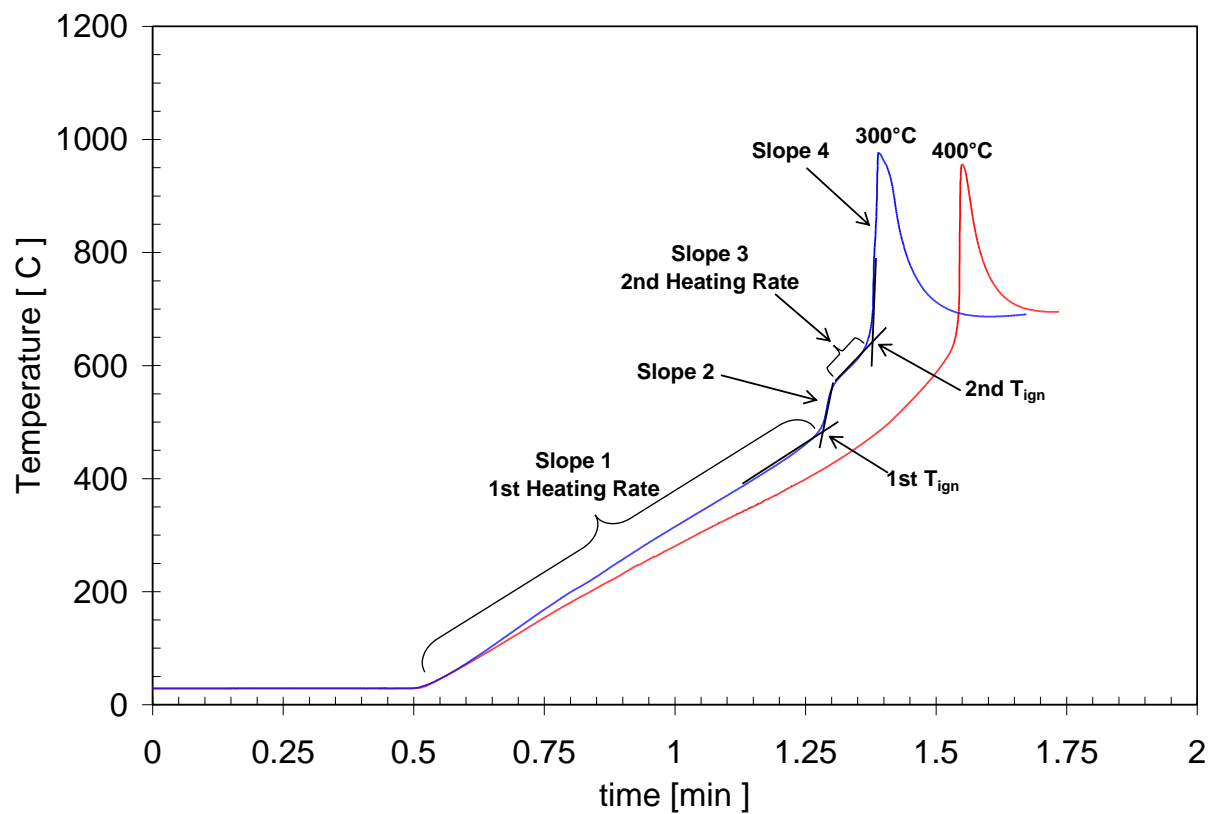


Figure 2. Shows a typical thermogram for Ta-WO<sub>3</sub> samples consolidated at 300 and 400°C. It also presents a schematic on the how the heating rate and the ignition temperature where determined with respect to the thermogram

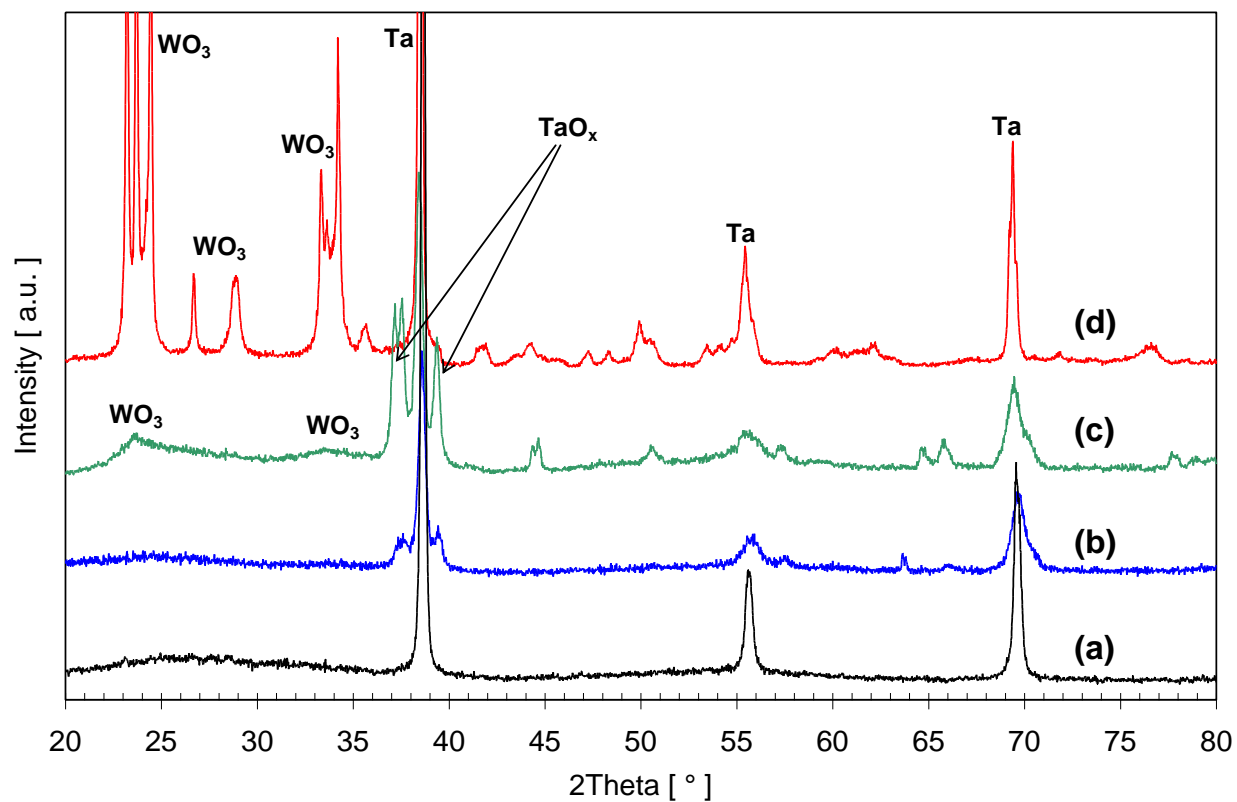


Figure 3. XRD patterns of (a) the starting SG derived Ta-WO<sub>3</sub> powder, (b) a 300°C as-consolidated SG Ta-WO<sub>3</sub> ground powder sample, (c) a 400°C as-consolidated SG Ta-WO<sub>3</sub> ground powder sample and (d) a non-consolidated (as-received) powder mixture of a commercially available WO<sub>3</sub> and Ta. The 300 and 400°C were consolidated using the HPSPS.

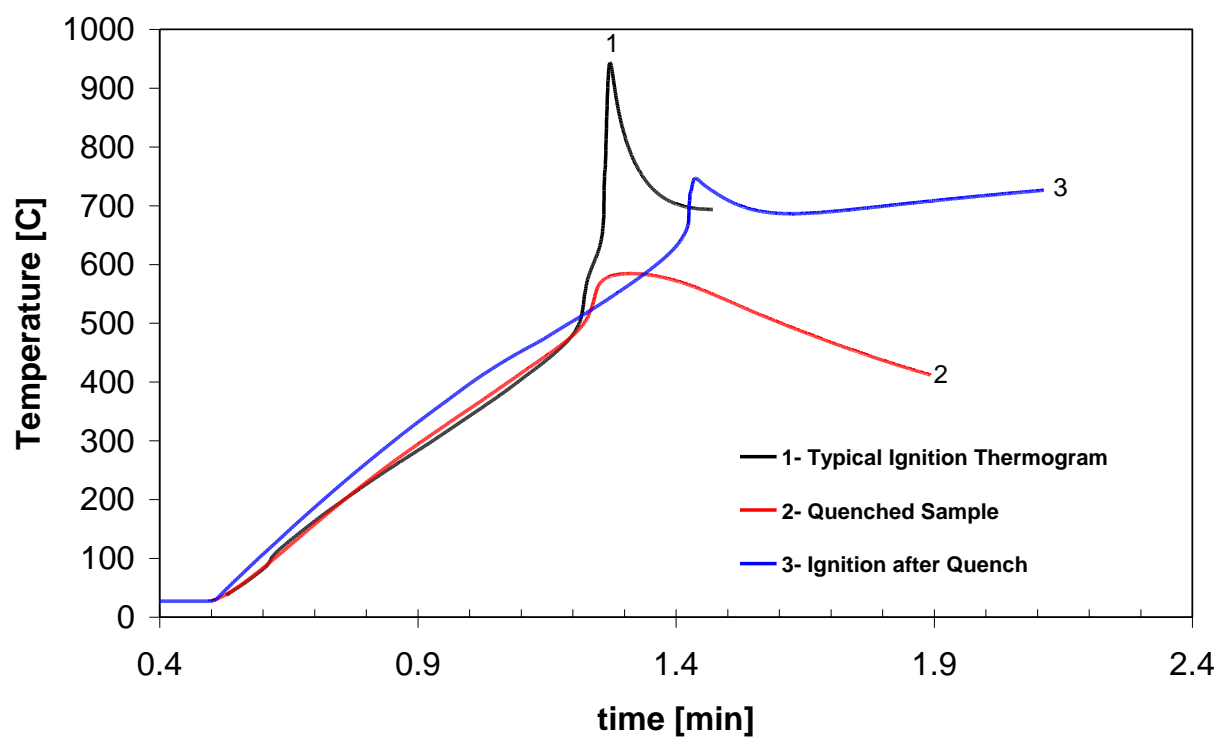


Figure 4. Thermograms for (1) a typical ignition for a 300°C SG Ta-WO<sub>3</sub>, (2) ignition quench of a 300°C SG Ta-WO<sub>3</sub> and (3) the ignition of the quenched 300°C SG Ta-WO<sub>3</sub> sample.

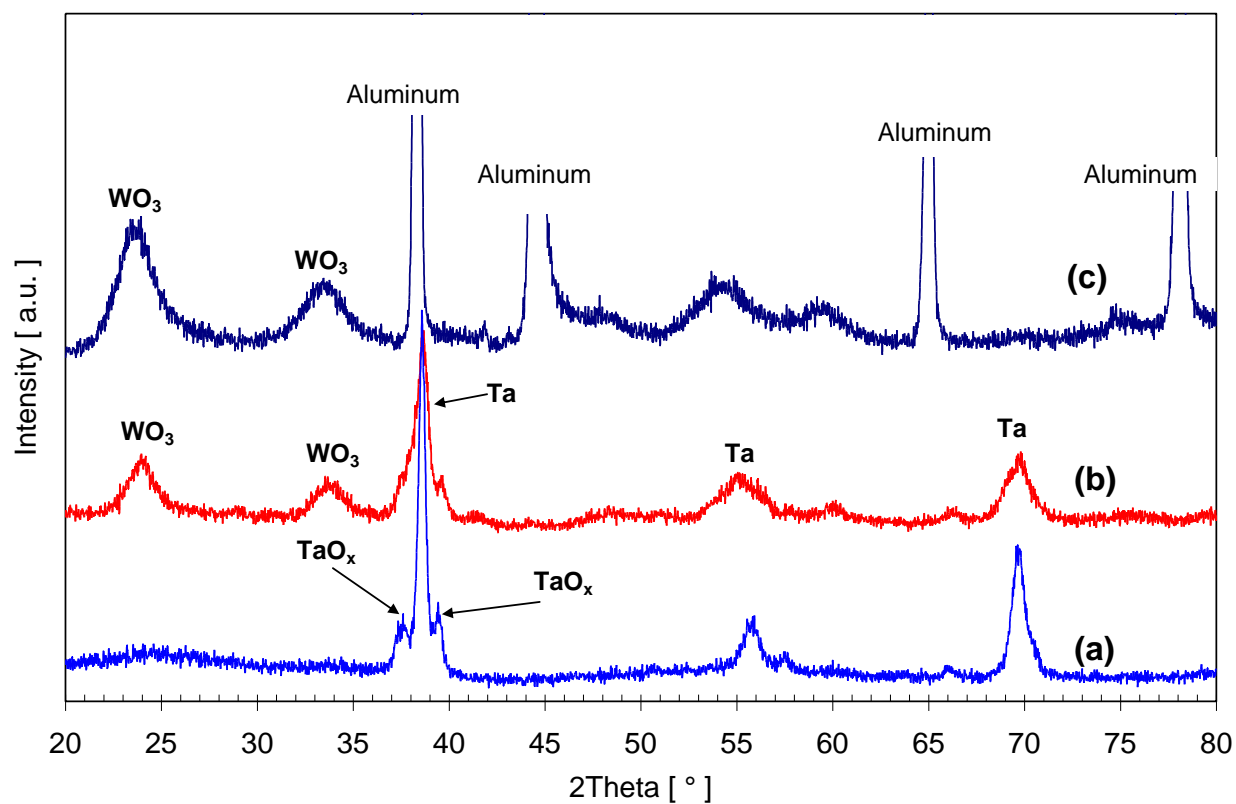


Figure 5. XRD patterns of (a) as-consolidated 300°C SG derived Ta-WO<sub>3</sub> pellet using the HPSPS to 300 MPa (b) quenched as-consolidated 300°C SG derived Ta-WO<sub>3</sub> pellet using the HPSPS to 300 MPa and (c) a quenched sol-gel amorphous WO<sub>3</sub> pellet pressed at 25°C and 300 MPa.

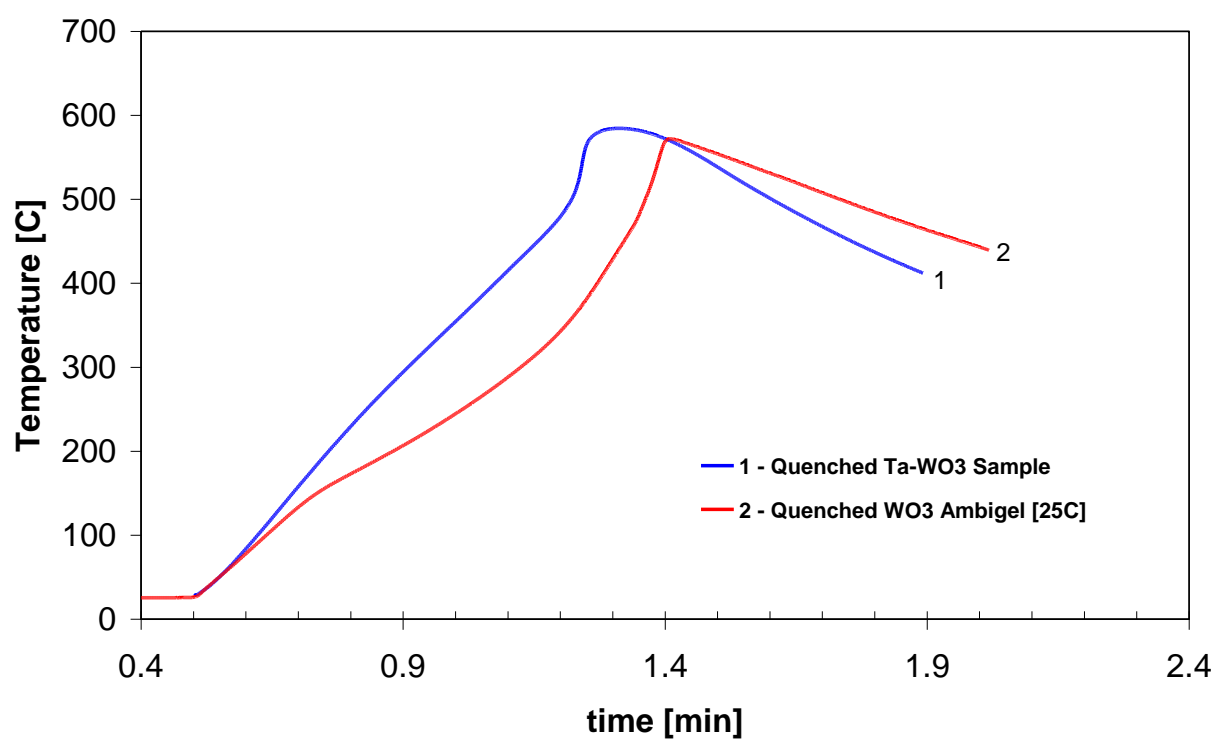


Figure 6. Quenched thermograms of (1) SG Ta-WO<sub>3</sub> and (2) sol-gel amorphous WO<sub>3</sub>. The SG Ta-WO<sub>3</sub> sample was pressed to 300°C using the HPSPS and the sol-gel amorphous WO<sub>3</sub> was pressed at 25°C. Both samples were pressed to 300 MPa.

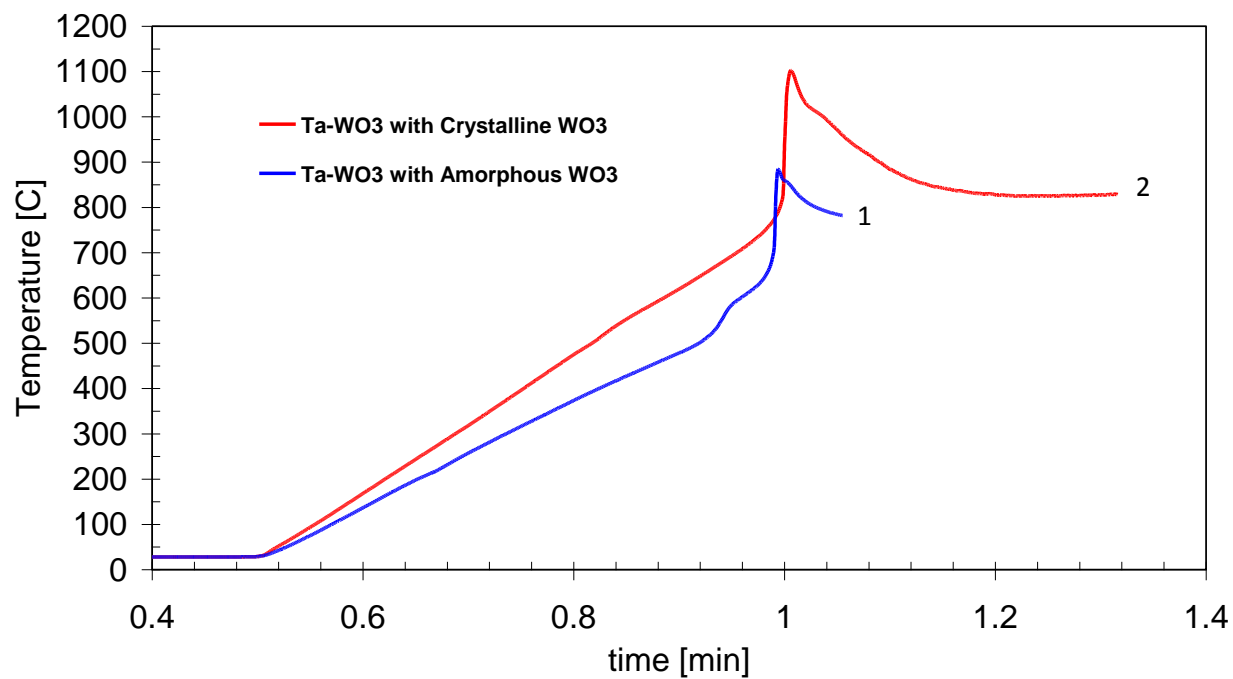


Figure 7. Typical ignition thermograms of (1) SG derived Ta-WO<sub>3</sub> composite and (2) Ta-WO<sub>3</sub> powder mixture with crystalline WO<sub>3</sub> when the furnace temperature is set 1000°C. Both samples were consolidated using the HPSPS to 300°C and 300 MPa.